



Internal cranial features of the Mojokerto child fossil (East Java, Indonesia)

Antoine Balzeau^{a,*}, Dominique Grimaud-Hervé^a, Teuku Jacob^b

^a*Equipe de Paléontologie Humaine, USM 204, UMR 5198, Département de Préhistoire du Muséum national d'Histoire naturelle, Paris, France*

^b*Laboratory of Bioanthropology, Faculty of Medicine, Gadjah Mada University, Yogyakarta, Indonesia*

Received 27 February 2004; accepted 21 January 2005

Abstract

The island of Java, Indonesia, has produced a remarkable number of fossil hominid remains. One of the earliest specimens was found in Pening and consists of an almost complete calvaria belonging to a juvenile individual, known as the Mojokerto child (Pening I). Using computed tomography, this study details its endocranial features. The specimen is still filled with sediment, but its inner surface is well preserved, and we were able to reconstruct its endocranial features electronically. The Mojokerto endocast is the only cerebral evidence available for such a young *Homo erectus* individual. We provide an analytical description, make comparisons with endocasts of other fossil hominids and modern humans, and discuss its individual age and taxonomic affinities. The ontogenetic pattern indicated by the Mojokerto child suggests that the growth and development of the *Homo erectus* brain was different from that of modern humans. The earliest stages of development, as characterized by this individual, correspond to important supero-inferior expansion, and relative rounding of the cerebrum. The following stages differ from that of modern humans by marked antero-posterior flattening of the brain and particularly antero-posterior development of the frontal lobes, resulting in the adult *H. erectus* morphology.

© 2005 Elsevier Ltd. All rights reserved.

Keywords: Endocast; *Homo erectus*; Mojokerto; Java; Indonesia; Ontogenesis; Development; Growth; CT

* Corresponding author. Antoine Balzeau, Département de Préhistoire du Muséum national d'Histoire naturelle, Institut de Paléontologie Humaine, 1 rue René Panhard, 75013 Paris, France. Tel.: +33 1 55 43 27 26; fax: +33 1 43 31 22 79.

E-mail address: abalzeau@mnhn.fr (A. Balzeau).

Introduction

The island of Java, in Indonesia, is a centre of extraordinary paleoanthropological interest. The first discoveries date back to 1891 when crews working for Eugène Dubois found fossils at Trinil that he attributed to *Pithecanthropus erectus* (Dubois, 1894). Since then numerous other field projects were undertaken throughout the island. Among the oldest specimens is the nearly complete calvaria of a young individual from Pening (von Koenigswald, 1936). The “Mojokerto child” could be as old as 1.81 Ma (Swisher et al., 1994) and, together with the Dmanisi fossil record (Gabounia and Vekua, 1995; Gabounia et al., 2002; Vekua et al., 2002; Antón, 2003), would represent some of the earliest evidence of hominid dispersal outside of Africa.

Pening I consists of an almost complete immature calvaria, including parts of the orbital plates and both petrous temporals; missing elements include the right portion of the frontal torus, the inferior region of the parietals, the squamous part of both temporals, and the lateral and the inferior portions of the occipital bone (for an exhaustive description of the individual, see Antón, 1997).

There are many discussions concerning the stratigraphical position and absolute age of Pening I (e.g. Hyodo et al., 1993, 2002; Swisher et al., 1994; Huffman and Zaim, 2003). On the whole, investigation of original archival records, and the evidence from subsequent fieldwork, support the conclusion that the calvaria was found *in situ* in the Upper Pucangan Formation (Duyfjes, 1936; Huffman, 2001). With special reference to this aspect, de Terra (1938: 4), who also compared directly the matrix in the calvaria and the sediment from the site, stated that “*in spite of the shallowness of its position there is nothing to cast a shadow of doubt on the stratigraphic position of the skull*”. By absolute dating pumice pebbles and hornblende sand coming from the same site but from the underlying horizon (Huffman and Zaim, 2003), Swisher et al. (1994) have proposed an age for the Mojokerto child of 1.81 ± 0.04 Ma. However, there is no evidence that the hominid specimen and the dated matrix are contemporary.

Even if the stratigraphical position of the fossil is certain, the volcanic sediment could have been reworked during the erosion of the volcano, and could therefore be older. Nonetheless, the reversed magnetic polarity of the volcanic sediments shows that this layer certainly precedes the Brunhes/Matuyama boundary (Sémah, 1986). Therefore, the absolute age of the Mojokerto child must be between 0.78 Ma and ~ 1.81 Ma.

A long time after its discovery, the taxonomic attribution and developmental age of the Mojokerto child are still in debate. Major difficulties come from the incomplete and immature nature of the specimen, and the lack of adequate comparative material. Historically, this individual was identified as *Homo soloensis* (Dubois, 1936), *Australopithecus* (Campbell, 1973), *Pithecanthropus modjokertensis* (Jacob, 1975; Sartono, 1975), *H. erectus* (e.g. Risçutia, 1975; Storm, 1994; Antón, 1997), and even *H. sapiens* (Weinert, 1938). The age at death estimates fluctuate between 1 year to over 8 years (Dubois, 1936; Weinert, 1938; von Koenigswald, 1940; Risçutia, 1975; Antón, 1997; Coqueugniot et al., 2001, 2004). Recent studies have concluded that the Mojokerto child is best considered as *H. erectus* based on cranial features shared with adult specimens belonging to this species (Storm, 1994; Antón, 1997).

The matrix filling precludes one from viewing the endocranial cavity and the internal features of the Mojokerto child (Fig. 1). Computed tomography (CT) enabled us to study the state of preservation and the degree of deformation of the calvaria and its endocast (reconstructed electronically in this study), as well as details of suture closure and internal cranial features (Fig. 2), including the bony labyrinth and other osseous structures. We present a detailed analytical description of the endocranial cast of Pening I, and make comparisons with endocasts of other fossil hominids and modern humans. Furthermore, as the growth and developmental patterns in *H. erectus* are still poorly documented (see Thompson and Nelson, 2000; Dean et al., 2001), we contribute to this key topic by assessing brain development during ontogeny in an early representative of this fossil taxon.

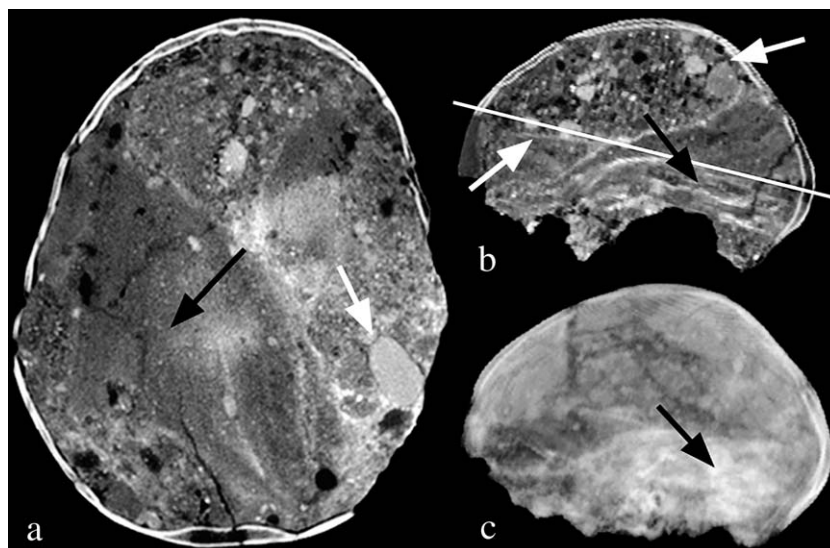


Fig. 1. (a) Transverse, and (b) midsagittal CT scans, and (c) a volume-rendered 3D reconstruction of Mojokerto, showing the stratification of the sediments inside the Mojokerto calvaria. In 'b' the white line indicates the position of 'a'. White arrows indicate coarser sedimentation and black arrows finer one.

Material and methods

For the purposes of the present study, the calvaria was CT scanned with a General Electric High Speed HAS scanner at the “CHNO des Quinze-vingts” in Paris (120 kV, 80 mAs, scan time 3 s). The full three-dimensional image stack consists of 112 contiguous, 1 mm thick slices in the coronal plane. The images have a pixel matrix of 512×512 , and with a field of view (FOV) of 23 cm the pixel size is 0.45 mm. The CT scans do not show any noticeable artifacts such as beam hardening or scattering even though the calvaria is heavily mineralized.

The use of CT in anthropological research began nearly twenty years ago. In spite of the technical limits of the earlier equipment, pioneer researchers (e.g. Tate and Cann, 1982; Wind, 1984; Vannier et al., 1985; Zonneveld and Wind, 1985; Ruff and Leo, 1986) were attracted by the opportunity to get access to the hidden structures of fossils. Since then, this remarkable technological enhancement produced numerous and diverse applications (e.g. Hublin et al., 1996; Spoor et al., 2000, 2003; Ponce de León and Zollikofer, 2001; Baba et al., 2003; Bookstein et al., 2003; Silcox,

2003; Bräuer et al., 2004; Rook et al., 2004), including attempts to estimate the endocranial volume (e.g. Conroy and Vannier, 1985; Conroy et al., 1990, 1998; Falk, 1998; Recheis et al., 1999; Tobias, 2001; Prossinger et al., 2003).

The CT data set was visualized and analysed using eFilm 1.8.1 and Mimics 7.1 software. Following previous work (Balzeau et al., 2002a,b, 2003a,b), we used the data to extract information concerning both the endocranial cavity, and the detailed morphology of the internal structures of the Mojokerto calvaria (Figs. 1 and 2). The method of using global thresholds of CT (Hounsfield) values to separate bone, sediments and air cannot be applied reliably to the Mojokerto CT scans, because their density ranges overlap, and part of the sediments would be included as bone, and part of the bone as sediments. We therefore developed a specific protocol to define the exact position of the different interfaces in order to obtain the most accurate results. On each CT slice, the boundary between the fossil and the filling sediment was identified by manual segmentation. This procedure consists of measuring the median value (or Half Maximum Height, HMH) from the CT value of the two

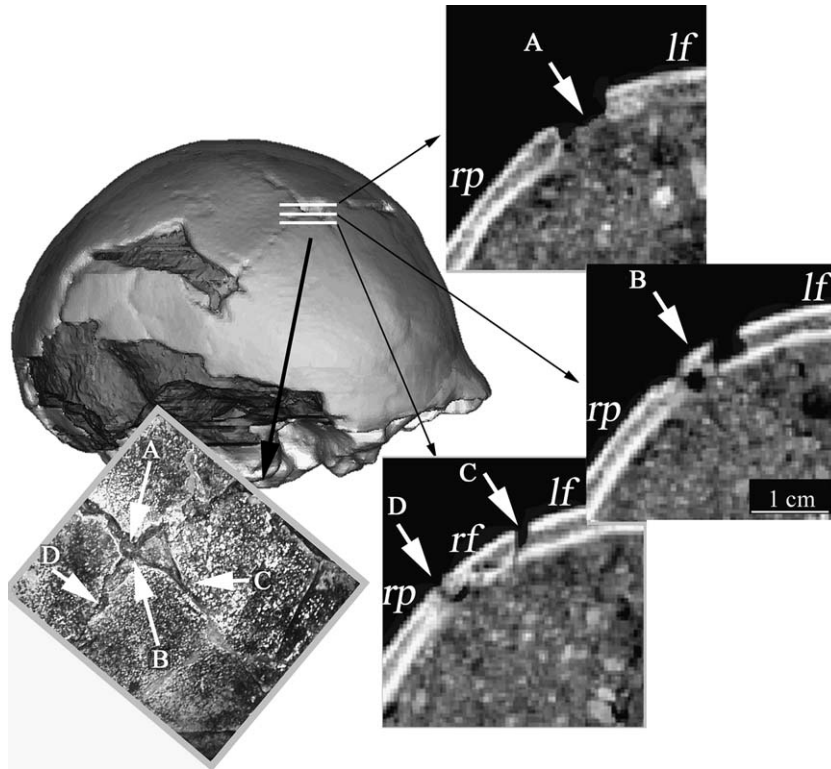


Fig. 2. Morphology of the anterior fontanelle of Mojokerto. The position of the three oblique CT sections (left posterior to right anterior) are indicated on the three-dimensional image. A anterior fontanelle, B osseous fragment, C fracture, D right coronal suture, *rp* right parietal, *rf* right frontal, *lf* left frontal.

elements (the fossil and the sediment) of which the interface should be defined (Spoor et al., 1993; Schwartz et al., 1998; Balzeau et al., 2002c). As the Hounsfield numbers of the matrix are lower than those of the fossilized bone, this value is used as the maximal one of the mask characterizing the endocast. This adjustment has to be made each time the attenuation coefficient of one of the elements varies all along the interface and on each CT slice. We named this protocol SMM (*Seuillage Manuel Multiple for Multiple Manual Thresholding*). It is time consuming, but it allows for accurate identification of the interface between two structures, despite local fluctuation in CT numbers. Finally, the boundaries obtained by the SMM protocol were used to calculate three-dimensional reconstructions of the endocast and the cranium.

The accuracy of the surface reconstructions are mainly determined by the spatial resolution of the CT data set, which is adequate to visualize vascular, sulcal and gyral impressions of the Mojokerto endocast (Fig. 3). Thus, the slice thickness and pixel size used here are a good compromise between obtaining sufficient spatial resolution, and the time-consuming process of isolating the virtual endocast.

We analysed the vascular, gyral and sulcal impressions of the Mojokerto child's endocast and compared its morphology with that observed on endocasts of fossil hominids and modern humans. The fossil sample includes *H. erectus* from Asia (N = 22 from Trinil, Sangiran, Zhoukoudian, Ngandong and Sambungmacan), Neanderthals (N = 10), and fossil *H. sapiens* (N = 9) (Grimaud-Hervé, 1997; Balzeau et al., 2002a,b). The

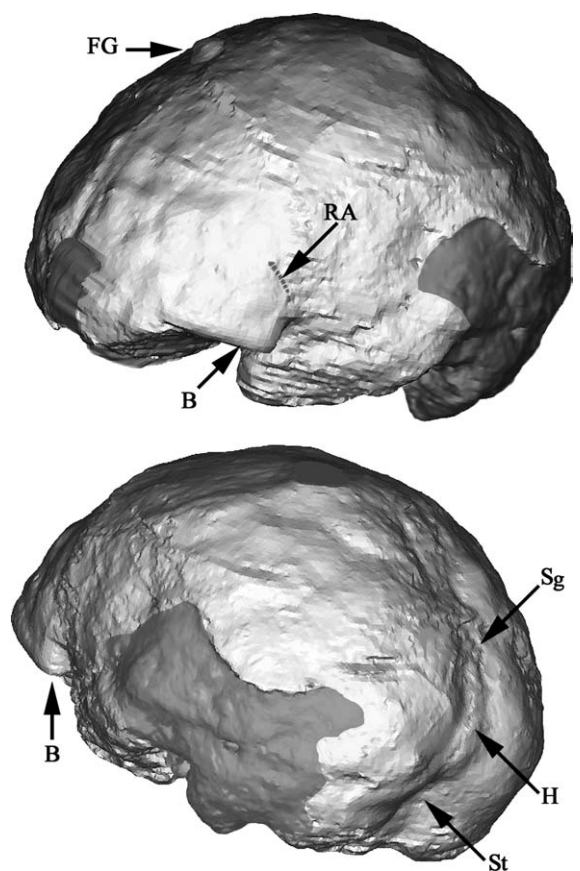


Fig. 3. Supero-lateral and postero-lateral three-dimensional visualization of the Mojokerto endocranial surface. FG granular foveola, RA ascending ramus, B Broca's area number 44 and 45, Sg superior sagittal sinus, H confluence of sinuses, St left transverse sinus; the maximum length of the endocranial surface is 128 mm.

modern human sample consists of 20 virtual endocranial surfaces obtained from CT data of 1.5 to 13-year old children (Bosma collection; Shapiro and Richtsmeier, 1997) and 30 adult physical endocranial surfaces all of unknown geographic origin (coll. Musée de l'Homme; DGH personal data).

Previous studies have shown that metric analyses of endocranial surfaces provide little useful information regarding the differences between fossil hominids and modern humans (Holloway, 1981; Grimaud-Hervé, 1994, 1997). Moreover, direct absolute metric comparison of the Mojokerto individual with *H. erectus* adult specimens and modern humans were not conducted because of its young

age at death. Geometric morphometric analyses are still in progress.

Results

Preservation

The CT images and the 3D reconstructions show detailed morphological features of the endocranial surface, such as some parts of the pattern of meningeal vessels and the gyral and sulcal imprints. This proves that the inner surface of the Mojokerto calvaria is well preserved. Interestingly, some bony fractures visible on the CT images extend also into the sediment. Consequently, it appears that the sediment filled the cranium before the specimen underwent substantial structural changes because of postdepositional taphonomic dynamics. Where parts of the vault bones are missing the endocranial surface has kept its original shape, suggesting that these parts were lost after fossilisation, and perhaps even during collection/preparation of the specimen (Huffman and Zaim, 2003).

The CT data shows a heterogeneous sediment inside the cranium (Fig. 1). The deposit shows a stratification of two layers: a coarser one, located antero-superiorly, and a finer one. Some elements contained in the sediment are spherical with a diameter close to 2 cm, substantial compared to the dimensions of the specimen, and probably correspond to pumice balls. No element of the sediment seems to represent bone from the cranium itself. The specimen seems to come from a high-energy fluvial sediment (Huffman and Zaim, 2003). However, the action of the water did not disarticulate the still unfused bones of the vault (Fig. 1). Also, the relatively sharp morphology of some free bony margins (*i.e.*, the lateral part of the supraorbital torus, the preserved regions of the basis) shows that any transport was short and that burial was fast. Available evidence suggests that the sediment penetrated the cranium when it had just lost its base, and that the specimen was embedded quickly before being dislocated. Even though this indicates that the endocranial matrix

and the fossil are contemporaneous, this may not represent the age of volcanic material itself.

The specimen is slightly deformed: the left parietal bone is raised in its median part. A fragment of the right parietal is isolated from the main part by an area of missing bone. This fragment is rotated to a more vertical orientation, and the calvaria probably suffered slight pressure on its right side postmortem. In addition, the left parietal bone is anteriorly compressed onto the frontal bone, and both the right parietal and right half of the occipital are shifted slightly posteriorly. The preservation of the internal surfaces will be considered together with the endocast.

Only the left frontal sinus is preserved. It is long and flat due to a lateral extension and its volume is small (greatest width of 34 mm, height less than 13 mm). The temporal bones are incomplete. The petrous parts are partially preserved, as is the anteriormost part of the left squamous part. The CT images show that the bony labyrinth, the vestibule and the cochlea are entirely preserved on both sides, whereas both the external and internal acoustic meati are absent. The external and internal bony laminae, as well as the diploë, are well-differentiated in all vault bones. Similar diploic differentiation in all vault bones was observed in modern humans from our comparative sample from the age of 3.

Suture synostosis on the internal surface

The state of suture synostosis on the internal surface was examined using cross-sectional images extracted from the original CT dataset (Fig. 2). As some sediments partially filled the still unfused sutures and the inner cracks of the original specimen, these features appear on the 3D reconstruction of the endocast.

The coronal, sagittal and lambdoid sutures are clearly detectable, as is the anterior fontanelle. The region corresponding to the mastoid fontanelle is not preserved on either side. A fine marking along the mid-internal surface of the frontal bone could correspond to the metopic suture, but this imprint appears to be a bony surface crack (Fig. 2, C). Thus, this suture is fused on both the exocranial (Antón, 1997) and the endocranial parts of the

Mojokerto frontal bone. The open coronal suture is about 6 mm wide. The sagittal suture is visible along its extension, while the lambdoid suture has the least marked inner suture.

Fig. 2 illustrates the vault morphology of the bregma region. The posteriormost slice shows a separation between the posteromedial part of the frontal bone, and the anteromedial corner of the right parietal bone (Fig. 2, A). At the margins of both parietal bones the diploë is covered with cortical bone. This morphology is typical of *in vivo* apposition of bone matrix during normal periosteal growth in a suture. It appears then that the space in this region is not caused by damage, but represents a small anterior fontanelle. Both margins of the frontal bone show a broken edge in this region, but they conserved their original conformation at the coronal suture. On the intermediate slice, an isolated bony fragment is located above the region of the fontanelles and corresponds to localized post-mortem damage representing an isolated element of the most posterior tip of the right frontal bone (Fig. 2, B). On the anterior slice, a fracture extends between two frontal halves (Fig. 2, C), whereas the coronal suture is very clear (Fig. 2, D). This coronal suture is a narrow sutural space between the right parietal and the frontal. Surface detail of the original fossil shows the same features, with fragments of the frontal joined with the sediment by preservative around the anterior fontanelle.

Morphological description of the endocranial cast

Overall morphology

As mentioned above the calvaria shows some taphonomic deformation. However, the overall shape of the endocranial cavity is well preserved because the vault does not show major breakage, and unfused bones stayed in articulation.

In superior view, the groove of the superior sagittal sinus is clearly discernible, but partially covered by an imprint related to the sagittal suture (Fig. 4). In fact, the sediment went into this suture, thus forming a fine ridge. In the same view it is difficult to identify precisely the position of the maximal width of the endocast because the corresponding region is not entirely preserved on

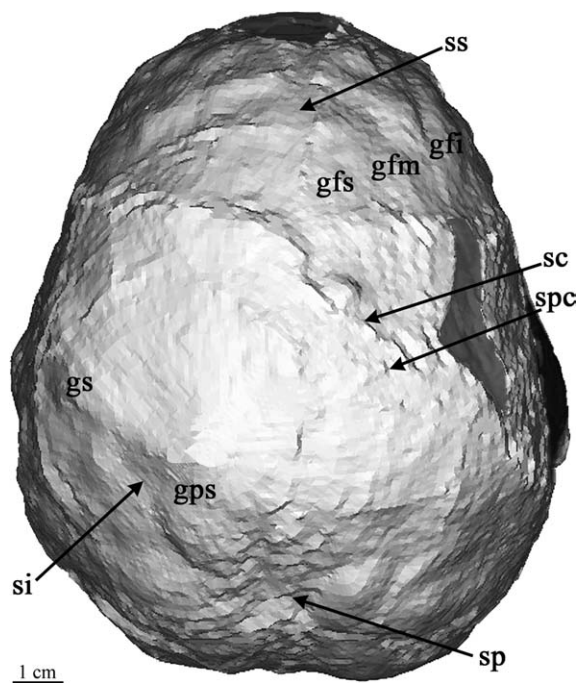


Fig. 4. Vertical view of the endocranium of Mojokerto. ss sagittal sulcus, gfs superior frontal gyrus, gfm medial frontal gyrus, gfi inferior frontal gyrus, sc central sulcus, spc post central sulcus, gps superior parietal gyrus, si intraparietal sulcus, gs supra-marginal gyrus, sp parietooccipital sulcus.

the left side. Nevertheless, it seems located in the posterior half of the endocranium. The preserved parts of the frontal lobes show a similar extension (no frontal petalia), while the right occipital lobe slightly extends posteriorly to the left one (occipital petalia) (Fig. 4). This last may be due to the taphonomic posterior slight shift of the occipital bone.

In lateral view (Figs. 7 and 8), the outline of the endocranium is regularly curved as far posteriorly as midway between bregma and lambda, with a more flattened area further posteriorly, which corresponds to the marked supralambdoid flattening on the outer surface. The endocranium maximal height is located in its median part. The curvature of the occipital lobes is unchanged.

In frontal and occipital view (Figs. 5 and 6), the two parietal lobes are similar in their rather straight outline superiorly, which makes an angle with the straight, and a sub-vertical outline

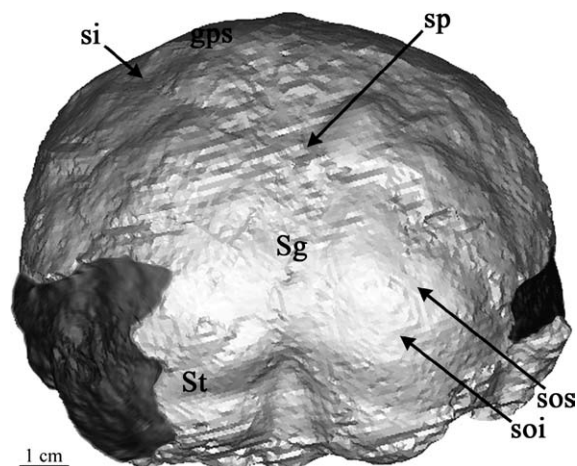


Fig. 5. Occipital view of the Mojokerto endocranium. gps superior parietal gyrus, si intraparietal sulcus, sp parietooccipital sulcus, Sg superior sagittal sinus, St left transverse sinus, sos superior occipital sulcus, soi inferior occipital sulcus.

more inferiorly. The base of the endocranium is better preserved on the left hemisphere. The maximum width of the endocranium is positioned inferiorly.

Vascular impressions

Venous sinuses. The groove of the superior sagittal sinus cannot be observed between the frontal lobes, but is visible in the posterior region of the parietal lobes beneath the imprint of the sagittal suture that covers it. It is visible again posteriorly between the endolambda and the endinion (Fig. 3, SS), where its width lessens (less than 8 mm) with respect to the anterior tract (average width of 10 mm). The sinus deviates laterally to the left into the left transverse sinus (Fig. 3, SL). No evidence of a transverse sinus is visible on the right hemisphere (Fig. 5). The region between this confluence of sinuses and the most basal available limit of the basi-occipital is well preserved, yet there is no indication of the presence of an occipital or a marginal sinus. The bilateral areas, where the pretrosquamosal sinuses should be found, are badly preserved and there is no trace of the sinus. On both sides, the sphenoparietal sinuses seem to be absent, but the morphology of the corresponding

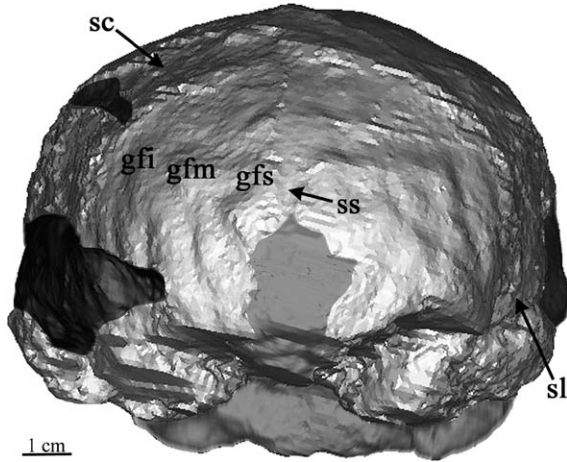


Fig. 6. Frontal view of the Mojokerto endocranium. ss sagittal sulcus, gfs superior frontal gyrus, gfm medial frontal gyrus, gfi inferior frontal gyrus, sl lateral sulcus, sc central sulcus.

region is affected by the imprint left by the coronal suture (Figs. 7 and 8). The sigmoid *sini* locations are not preserved.

Granular foveola. An imprint is present on the right hemisphere, near the sagittal suture, 12 mm behind the coronal suture. This imprint erodes the internal cranial surface at a thickness of 2 mm and forms a depression consistent with a granular foveola, visible on the two-dimensional CT

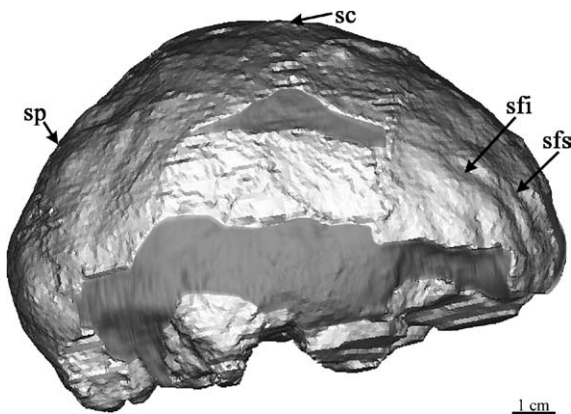


Fig. 7. Right lateral view of the Mojokerto endocranium. sfs superior frontal sulcus, sfi inferior frontal sulcus, sc central sulcus, sp parietooccipital sulcus.

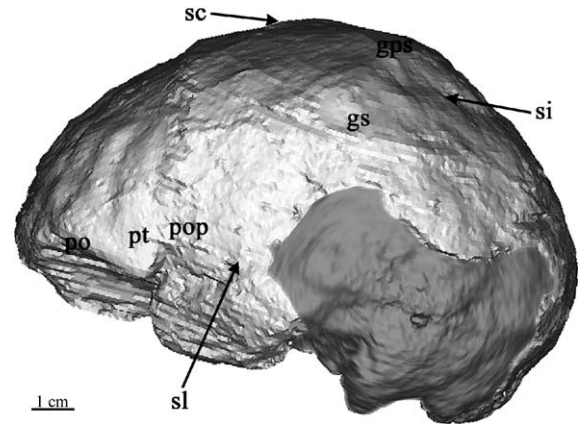


Fig. 8. Left lateral view of the Mojokerto endocranium. po orbital part, pt triangular part, pop opercular part, sl lateral sulcus, sc central sulcus, gps superior parietal gyrus, si intraparietal sulcus, gs supramarginal gyrus.

images. This feature has a circular shape with a diameter of 8 mm (Fig. 3, FG).

Meningeal vessels. The surface of the frontal lobes is well preserved anteriorly to the coronal suture, but there are no traces of the anterior meningeal vascular system (Fig. 6). Cracks on the internal bony surface appear at the level of the parietal lobes. They constitute a fine network on the endocranial surface of well-defined structures that are less than a millimeter in width, and are not observable ectocranially. The presence of sediment and the alterations it caused on the internal surface may be the reason for poor preservation of the features corresponding to the middle meningeal network on the parietal lobes. However, a portion of the anterior meningeal artery is preserved on the left hemisphere (Fig. 8). Where it runs obliquely posteriorly and superiorly extending 20 and terminates less than 1 cm from the interhemispheric limit. It disappears inferiorly as it approaches the coronal suture. On this same hemisphere, a 50 mm long branch of the posterior meningeal artery has the same direction as the branch of the anterior meningeal artery. An imprint of the same branch extends over 26 mm symmetrically on the right hemisphere. These two posterior

meningeal branches extend almost as far as the interhemispheric limit (Fig. 4).

Gyral impressions

The sagittal sulcus forms a slight depression posterior to the endoglabella and extends vertically as far as the endobregma (Fig. 6). The central sulci are visible, especially near the sagittal region. In their connection, the imprint left by the sagittal suture stands out in a slight depression (Fig. 4). On the right hemisphere, the central sulcus extends just posteriorly to the granular foveola (Figs. 4 and 7). As the fontanelle is open, it is difficult to localize precisely the position of the endobregma. The endolambda is also not easy to localize because the sagittal and lambdoid sutures are wide at their junction. Thus, the connection of the central sulci is located approximately 29 mm from endobregma and 62 mm from endolambda.

The frontal and temporal lobes are separated at the lateral sulcus starting point by a wide and deep depression that goes on posteriorly by a short oblique depression on the left hemisphere (Fig. 8). The corresponding region is not preserved on the right hemisphere (Fig. 7). On the two hemispheres, the ascending ramus is visible (Fig. 3).

On the right hemisphere, the parietooccipital sulcus forms a brief and light depression anteriorly to the lambdoid suture (Fig. 7). The corresponding region on the opposite hemisphere, which does not present any track of this sulcus, is distorted because of the upthrust of the parietal bone anteriorly to the lambdoid suture.

Sulcal impressions

Right frontal lobe (Fig. 7). On the two-dimensional CT images it appears that the ethmoid and the sphenoid bones are damaged, and the basal parts of the frontal lobes are not well-preserved. The most anterior region of the lobe is absent and the inferior surfaces of the frontal lobes are damaged. The bulge formed by the coronal suture in relief and the raised parietal bone make the precentral sulci barely recognizable on both sides (Fig. 4). As a result, the width of the precentral gyri cannot be assessed accurately. The superior frontal sulcus is slightly marked and regularly

curved from the most anterior preserved part of the frontal lobe. It goes as far as the coronal suture by moving away from the interhemispheric limit. The superior frontal gyri have a comparable width on both hemispheres. The inferior frontal sulcus is very marked and slightly sinuous and is preserved to the coronal suture. The middle frontal gyri are wide on both hemispheres. The external part of the inferior frontal gyrus is rather complete missing only the orbital portion and the inferior region of the triangular portion. The preserved portion of the ascending ramus is tilted posteriorly and disappears at the level of the coronal suture. The opercular portion is not preserved.

Left frontal lobe (Fig. 8). The superior frontal sulcus and the inferior frontal sulcus are more sinuous than on the opposite lobe and delimit clearly the three frontal convolutions (Fig. 6). The ascending ramus and the anterior ramus are visible. The former is slightly tilted anteriorly and extends over 15 mm (Fig. 3, RA), while the latter curves upward. The cap incisure forms a rather wide and shallow depression. The so-delimited triangular part constitutes a well developed relief. This bulge corresponds to area 45 situated on the left inferior frontal gyrus and anteriorly to the ascending ramus (Fig. 3, B). It is localized anteriorly to the temporal pole from which it is separated by a wide and deep depression. The orbital part is complete anteriorly and extends antero-posteriorly to about 30 mm. Behind it, the surface corresponding to the opercular part obscured by the coronal suture. The inferior surface of the frontal lobe is complete but poorly preserved. A depression can be observed on its external part that might represent the external orbital gyrus.

Right parietal lobe (Fig. 7). This lobe is incomplete in its inferior part due to the partial preservation of the right parietal bone. A 44 mm triangular-shaped zone is missing along its median part, antero-posteriorly of the coronal suture. A crack runs from the superior limit of this break to join the sagittal suture. Two other cracks run inferiorly and isolate a bone fragment posterior to the coronal suture. The orientation of the corresponding

endocranial surface follows the detachment of this bony portion. There is little evidence of the anterior, posterior and inferior limits of this lobe on both hemispheres because of the incompleteness of the parietal bones; moreover, the sulci that define them are not perceptible along their whole length. The postcentral sulcus is visible on the superior part of the parietal lobe (Fig. 4). The postcentral gyri seem to be of comparable size. The transition between the postcentral gyrus and the superior parietal gyrus is marked by a slight depression of the sagittal suture imprint. The superior parietal gyrus is slightly wider on the right parietal lobe. The intraparietal sulcus, which runs toward the sagittal axis, constitutes a visible depression located just above the median break on the parietal bone. The supramarginal gyrus forms a light convexity. It seems difficult to define its limits because it is close to a break between two osseous fragments.

Left parietal lobe (Fig. 7). Its anterior surface is slightly heightened because of the post-mortem compression between the corresponding parietal bone and the frontal bone. The lower posterior part of this lobe is incomplete. The postcentral sulcus is more detectable than on the opposite hemisphere. The intraparietal sulcus shows a wide depression and is partially preserved anteriorly, where the postcentral sulcus is absent. The interparietal sulcus extends posteriorly in the direction of the superior edge of the parietal lobe. The supramarginal gyrus, which is crossed antero-posteriorly by an imprint corresponding to a crack in the temporal bone, is convex. The antero-inferior portion of the second parietal convolution is distorted and exhibits weak relief.

Temporal lobes. Only the most postero-superior part of the right temporal lobe is preserved and its various convolutions cannot be located (Fig. 7). The endocranial features of the left temporal lobe surface are not preserved (Fig. 8).

Occipital lobes (Fig. 5). The right side is more complete than the left side. The superior and inferior occipital sulcus are visible, the latter showing the same orientation on both hemispheres. As the

drainage of the superior sagittal sinus goes into the left transverse sinus, the third occipital convolution continues lower on the right hemisphere than on the left one. This also occurs because the right occipital lobe extends lower than the left one in occipital view. The third occipital convolution is bigger than the left one from superior to inferior.

In postero-superior view, this occipital lobe has a more pronounced posterior extension than the left one because of a slight antero-posterior occipital petalia. The transition with the cerebellum is not as clear as on the left hemisphere because of the disappearance of the right transverse sinus. On the left side only the inferior occipital sulcus is visible. It forms a shallow and very wide depression. Underneath this lobe, the transverse sinus is wide and prominent.

Cerebellar lobes (Fig. 5). These are poorly preserved, but are separated by a very wide and deep depression. No imprint can be seen on their surface. In lateral view (Figs. 7 and 8), the cerebellar lobes are located beneath the occipital lobes.

Endocranial volume

As the specimen is not complete, especially in the area of the basicranium, the volume of the three-dimensional reconstruction of the preserved endocranial cast of 595 cm³ is less than the actual cranial capacity of the Mojokerto child. Hence, in order to achieve the most realistic estimate of the cranial capacity a reconstruction of the missing parts was necessary. Sediments are present underneath the preserved parts of the parietal bones and anteriorly to the left side of the occipital bone. The corresponding bony parts probably disappeared after fossilization. Therefore, this sediment virtually presents the overall internal shape of the missing bony parts, even though the morphological features of the corresponding surface of the endocast are not preserved. Thus it is mainly portions of the basicranium from the basi-occipital and posterior of the temporal poles that require reconstruction.

The first step of reconstruction consisted of completing the right hemisphere: (1) the third frontal convolution, (2) the lateral and inferior

shape of the temporal lobe, (3) the posterior part of the temporal lobe, (4) the inferior portions of the occipital and the cerebellar lobes. This was possible by using the morphology of the more complete left hemisphere. Mirror imaging of the three-dimensional reconstruction and the curvature of the preserved portions were used to complete the missing sections. The second step was to reconstruct the basicranium in the foramen magnum region where a relatively small volume is missing. The variation in volume of the different possible reconstructions of this region is small, when compared with the total endocranial volume. The variation encountered in our different attempts to complete the missing parts of this endocranial cast was 13 cm³. In order to consider this variation as well as others factors (the slight deformation of the endocast, the inter-observer variation, the limitations of the medical imaging technique) we propose an arbitrary range of 20 cm³ to include the mean estimation of this individual endocranial cavity. The reconstruction of missing parts allows us to estimate a endocranial capacity of between 620 and 640 cm³. This value corresponds to the volume of the entire encephalon reconstruction. This method represents a direct and reproducible measurement, unlike methods based on estimations of the external cranial anatomy.

Discussion

The dentition of the Mojokerto child is not preserved, and methods based on the stages of dental eruption could not be used for age estimation. Moreover, methods based on suture closure specifically apply to modern humans, and are known to be unreliable (e.g. Masset, 1971; Ferembach, 1983; Hershkovitz et al., 1997). Applying the evidence derived from modern humans to an extinct species is obviously problematic. Von Koenigswald (1940) considered the Mojokerto child around 5 years old at death. Risçutia (1975) suggested an age of 2.5 years to 3.5 years, based on estimates of the specimen's adult endocranial volume. Antón (1997) proposed a developmental age between 4 and 6 years, based on

the morphology of the cranial base and vault, and making comparisons with development in Neanderthals and *Homo sapiens*. Finally, Coqueugniot et al. (2001, 2004) using CT scans of endocranial morphology suggested an even lower age of 1 year (range 0 and 1.5 years), based on the morphology of the tympanic, the subarcuate fossa and the anterior fontanelle, and statistical comparison with age series of modern humans, chimpanzees and bonobos.

We can now consider features revealed by the CT images and three-dimensional reconstructions to discuss the Mojokerto child's developmental age. However, this information appears to be not always internally consistent.

The closing of the fontanelles occurs very early in modern humans: the sphenoidal and posterior fontanelles disappear at the age of 2 or 3 months and the anterior fontanelle in the middle of the second year with significant individual variation (Paturet, 1951; Kamina and Renard, 1994; Scheuer and Black, 2000). The network of meningeal vessels might also indicate that this individual could be a young child. It has left very few imprints on the endocranial surface, either because the endocranial surface was only partially preserved during the fossilization process, or it could not have been completely imprinted yet at the individual's young age. Moreover, no trace of the anterior meningeal vessel was visible even though the corresponding surface of the endocast is very well preserved. The anterior meningeal vascularisation emerges in modern humans around the age of 6 (Saban, 1988), and its absence on the Mojokerto fossil would indicate a younger age.

On the other hand, the presence of a granular foveola and frontal impressions, as well as the development of the frontal sinuses would suggest an older age. The digital impressions are very numerous in the anterior region of the frontal lobe, and in modern humans these appear between 3 and 5 years (Saban, 1988). In the same way, granulations are rare and weakly developed in *Homo sapiens* children. They grow in number and size with age during adulthood (Grimaud-Hervé, 1997). In modern humans the expansion of the frontal sinuses takes place at an age corresponding to the eruption of the first molar (Hauser and

de Stefano, 1989; Minugh-Purvis et al., 1999). Moreover, the air cells do not reach the level of the superior orbital margins before 7 to 8 years of age (Koppe and Ohkawa, 1999). In *Gorilla gorilla*, the frontal sinuses emerge after completion of the primary dentition and pneumatizes the frontal bone at the eruption of the maxillary first molar (Cave, 1961). The left sinus observable in the frontal torus of Mojokerto was a thin channel spreading parallel to the bony tables. It has a comparable development to modern human children around the age of 8–9 (Libersa and Faber, 1960).

Supraorbital prominences are present on the Mojokerto fossil. In modern humans, the emergence of the supraorbital structures take place at the time of puberty (Weinmann and Sicher, 1955). However, these structures are slightly developed on the Mojokerto fossil compared to the morphology of an adult *Homo erectus*. This evidence does not allow us to exclude a young age for this individual, but shows that *Homo erectus* and *Homo sapiens* do not share the same rate of frontal superstructures development.

This individual has an endocranial capacity of 630 cm³ while modern humans have an average volume of 567 cm³ at 4 months and 803 cm³ at 1 year (N = 33792 and N = 31596 respectively, data are from the U.S. Perinatal Project, after Rushton, 1997). The Mojokerto child would therefore have had an endocranial capacity in the modern human range if he was less than 1 year old (after Coqueugniot et al., 2001, 2004). If true, it would then imply either a neonatal endocranial volume in *Homo erectus* comparable with modern humans or a faster brain growth rate during *Homo erectus* infancy. Based on our reconstitution, Mojokerto has an endocranial capacity at about 52–79% of adult *Homo erectus* variability (respectively for adults values ranging between 1200 and 800 cm³). For comparison, modern humans have a value of 59.5% of adult endocranial capacity at 1 year (based on values from Beals et al., 1984 and Rushton, 1997), and chimpanzee have a 80% adult volume at the same age (Coqueugniot et al., 2004). Based on these results, Mojokerto could follow the relative brain growth of chimpanzee if he were 1 year old, but also the relative brain growth of the

modern human at the same age or even older. If considering a brain developmental pattern intermediate between chimpanzees and modern humans (Bogin, 2003), this evidence does not allow the exclusion of an individual age older than 1 for Mojokerto.

Our data based on CT scanning of the Mojokerto child lead us to suggest that he was less than 4 years old when he died if we consider that its development followed nearly the same pattern and rate of growth as modern humans or even a faster rate. However, applying modern human growth standard to this unique representative of an *Homo erectus* child appear quite problematic as we have a very partial knowledge of ontogenetic mechanisms in this extinct species. Moreover, further investigations are needed in order to estimate timing of *Homo erectus* growth (e.g. Dean et al., 2001; Zihlman et al., 2004) before discussing in detail and precisely the Mojokerto individual age.

Previous estimates of the cranial capacity of the Mojokerto child, based on the external morphology, range between 636 and 700 cm³ (Dubois, 1936; Jacob, 1966; Risçutia, 1975), and our estimate of 620–640 cm³ falls at the lower margin. It is lower than the 663 cm³ obtained by Coqueugniot et al. (2004), the only other study which used CT to estimate the cranial capacity from the internal morphology. The discrepancy must be the consequence of differences in the reconstruction of the missing parts. Coqueugniot et al. (2004) reconstructed the missing portions of the base on reconstructed sagittal slices with 2 mm interval. We used here 1 mm thick slices and especially mirror imaging of the three-dimensional reconstruction and the curvature of the preserved portions to complete in 3D the missing parts.

Given its immature status, the endocranial capacity obtained for the Mojokerto child is compatible with its attribution to *Homo erectus*. Values obtained for adult *Australopithecus* rarely exceed 500 cm³ (Falk et al., 2000), and adult *H. habilis* and *H. rudolfensis* have an average volume of 634 cm³ (n = 7; Holloway, 1973, 1978, 1983a; Stringer, 1986). If the child had achieved adult growth he would have attained a cranial capacity in the adult Asian *Homo erectus* range of

variability, between 840 and 1245 cm³ for the fossils of Trinil, Sangiran and the *Sinanthropus* (n = 10; Grimaud-Hervé, 1997).

The superior sagittal sinus is continuous with the right transverse sinus in modern humans and most fossils assigned to the genus *Homo* (respectively 80 and 85%, Grimaud-Hervé, 1997). In the Mojokerto child it continues into the left transverse sinus (Fig. 3), as is the case in 20% of modern humans (with some variations e.g. Grimaud-Hervé, 1997; Bruner et al., 2003). The predominant presence of an enlarged occipital-marginal sinus in *Paranthropus robustus*, *P. boisei*, and *Australopithecus afarensis* is established (e.g. Tobias, 1987; Tobias and Falk, 1988; Saban, 1993; Falk et al., 1995). In adult *Homo erectus*, the superior sagittal sinus is continuous with the right transverse sinus in Trinil 2, Sangiran 12 and 17, Ckn.E 1.PA.16 (III), Ckn.L 1.PA.98 (X), Ckn.L 2.PA.99 (XI), Ckn.L 3.PA.100 (XII), Ngandong 6, 7 and 12, and with the left in Sangiran 2 and 10. Only Sambungmacan 3 shows an occipital-marginal sinus (Broadfield et al., 2001; Balzeau et al., 2002b). The presence of this feature on Trinil 2 is not confirmed (*contra* Falk, 1986). This endocast shows a preponderant right transverse sinus where the superior sagittal sinus continues in majority. The left transverse sinus is less printed. It is situated just above the preserved limit of the endocast and no relief in this region can be interpreted as an occipito-marginal sinus. This system is absent in Mojokerto, as is the most frequent condition in the genus *Homo*.

The asymmetric pattern of the transverse sinuses and the confluence of sinuses may be associated with the asymmetric development of one of the cerebral hemispheres (Delmas and Chifflet, 1950). In spite of the strong development of the left transverse sinus (Fig. 3, St), the endocast of the Mojokerto individual does not show a clear predominance of one of the hemispheres. The right one is larger and the occipital pole extend posteriorly to the left one in superior view, but this extension was certainly slightly amplified by the diagenetic processes that this fossil underwent.

The sphenoparietal sinus seem to be absent on Mojokerto, even if the corresponding areas are affected by the presence of the coronal suture. This

feature is variably present and slightly developed on the Trinil, Sangiran and Zhoukoudian endocasts. It is always absent on the Ngandong and Sambungmacan hominids and the actual modern humans sample (Grimaud-Hervé, 1997; Balzeau et al., 2002b).

The meningeal network left very few prints on the endocast. No trace of the anterior meningeal vessel was visible whereas the corresponding surface is very well preserved. Meanwhile, a granular foveola is visible in the posterior part of the right frontal lobe, close to the sagittal sulcus. In modern humans these granulations are absent in foetuses, rare and less developed in children. They increase in number while the cerebral volume increases with age. Therefore, the important development of this feature on Mojokerto might indicate a faster vascular development of the brain than in modern humans. In adults *Homo erectus*, granular foveolae are very frequent on the posterior part of the frontal lobes in the Trinil, Sangiran and Zhoukoudian fossils and less in the Ngandong and Sambungmacan hominids. These features are more numerous and developed in these adults than on the Mojokerto endocast.

In modern humans, Broca's motor and speech area is composed of areas number 44 and 45 (Bouret and Louis, 1974; Grimaud-Hervé, 1997). On the Mojokerto endocast, there is a bulge corresponding to area 45 situated on the left inferior frontal gyrus and anteriorly to the ascending ramus (Fig. 3, B). The presence of this feature is variable in australopithecines (Tobias, 1975), and appears more consistently in *H. habilis* and *H. erectus* (Holloway, 1983b; Tobias, 1983; Broadfield et al., 2001). Its relevance as evidence for the existence of some hypothetical language facilities is dubious (Maitre Robert, 2002). However, this relief has a similar development and the same localization relatively to the temporal lobe in Mojokerto than in Asian *Homo erectus*. Similarly, they all present a wide and deep depression at the origin of the lateral sulcus.

The overall shape of the frontal lobes in anterior view is characteristic of various groups of hominids (Grimaud-Hervé, 1997). Outlines which correspond to the orientation of the inferior surface of the frontal lobes and the encephalic

rostrum show a regular curvature in the case of the endocasts of the Trinil, Sangiran and Zhoukoudian hominids. Ngandong and Sambungmacan endocasts show a clear discontinuity between these two planes, as it becomes more oblique in later representatives of the genus *Homo*. In Mojokerto the encephalic rostrum region is not preserved, but the left frontal lobe is similar to that of the Zhoukoudian, the Trinil and the Sangiran specimens (Fig. 6). This morphology indicates a relative low development of the prefrontal cortex in comparison with that observed in *Homo sapiens*. Indeed, the inferior part of the inferior frontal gyrus in the Mojokerto child is similar in shape and development to all the Asian *Homo erectus* except the Ngandong and Sambungmacan individuals (Grimaud-Hervé, 1997; Balzeau et al., 2002a,b).

The Mojokerto specimen is similar to *Homo erectus* from Trinil, Sangiran and Zhoukoudian in that the anterior-inferior part of the second parietal convolution shows weak relief, the supra-marginal gyri are not prominent, the occipital lobes are separated by a wide inter-hemispheric space, and are located behind the extension of the parietal and temporal lobes, and the cerebellar lobes are prominent, separated by a large groove and located underneath the occipital lobes. All these features show a continuous shift in direction of modern human morphology during hominid evolution (see Grimaud-Hervé, 1997 for an exhaustive description of these transformations). The Ngandong and Sambungmacan endocasts have a particular morphology for these features (Grimaud-Hervé, 1997; Balzeau et al., 2002a,b), not shared by others Asian *Homo erectus* nor the Mojokerto individual.

Consequently, all these vascular and gyral features suggest closer affinities for the Mojokerto child with the Trinil, Sangiran and Zhoukoudian *Homo erectus* while the Ngandong and Sambungmacan fossils present a relatively more evolved morphology (Grimaud-Hervé, 1986, 1997; Balzeau et al., 2002a,b).

The orientation of the ascending ramus, compared to the posterior ramus, varies among hominids. It is quite vertical on the Asian *Homo erectus* endocasts but goes forward in modern

humans; a change correlated with the anterior shift of the frontal lobes. The ascending ramus is slightly tilted forwards on the Mojokerto left hemisphere (Fig. 3, RA), showing some similarity with modern humans. This is due to the relative height and convexity of the endocast in the lateral view (Figs. 7 and 8) and particularly to the frontal lobes anterior rounding. Indeed, the corresponding endocranial outline is more globular than seen in any adult *Homo erectus* individuals. On the Mojokerto endocranial cast, the connection of the central sulci is located in the anterior third of the endobregma-endolambda axis. This position is similar to that in modern humans while the Sangiran, Trinil, and Zhoukoudian endocasts have a connection situated at the 2/5 of this axis (Grimaud-Hervé, 1997). Thus the parietal lobes of Mojokerto are relatively more developed than those of its contemporaries and the frontal lobes show a relatively less antero-posterior extension. This individual differs from adult *Homo erectus* in the position of the endocranial vertex because it is located near the central sulci intersection. The Mojokerto cerebral shape would have got longer and flatter during growth making it more similar to adult individuals. These modifications are particularly characterized by an antero-posterior development of the frontal lobes and associated compression of the parietal lobes. Alternatively, the cerebrum increases in height between modern human children and adults resulting in cerebral rounding. This suggests that *Homo erectus* had an ontogenetic pattern that differed from the modern human pattern.

Studies of young modern human endocasts show that the digital impressions appear on the frontal lobes between 3 and 5 years (Saban, 1988). The digital impressions are numerous on the anterior region of Mojokerto's frontal lobes, whereas the anterior fontanelle and sutures are distinctly unfused. The imprints on this endocast are more developed than in most adult *Homo erectus* specimens and than those in chimpanzees regardless of their developmental stage. They are similar to those observed for 6-year-old modern humans in our comparison sample (Fig. 9). This should not be considered as a diagnostic feature for modern humans, but rather as the consequence

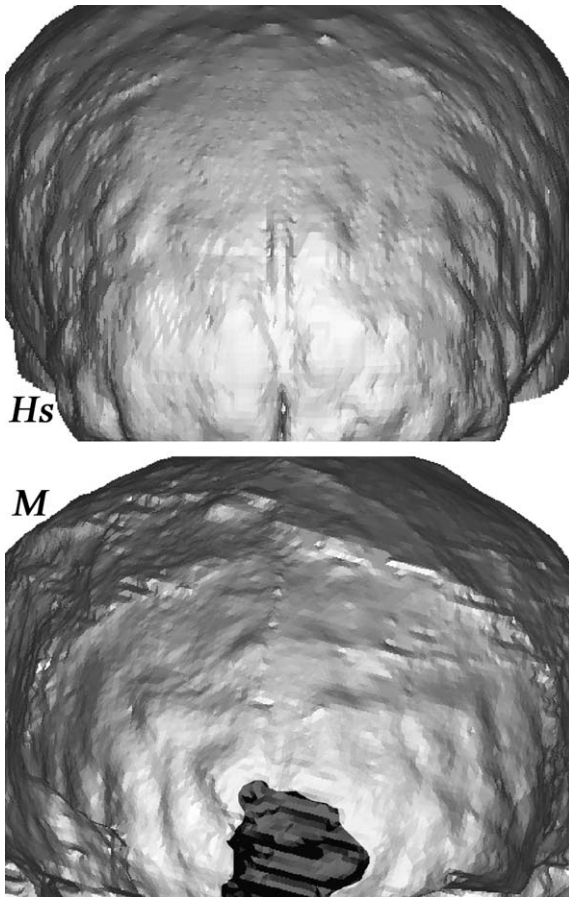


Fig. 9. Details of the digital impressions on the frontal lobes on a 6 years old modern human (top, Hs) and on the Mojokerto endocranial cast (bottom, M).

of the young age of this fossil child. The preponderance of this feature on Mojokerto compared with adult *Homo erectus* is due to brain growth trajectory in this extinct species. The earliest stages of development, as characterized by this individual, correspond to an important vertical development and a cerebral rounding. This implies a significant pressure of the frontal lobes against the frontal bone, causing these digitations. The transformation to an adult morphology occurs by an antero-posterior flattening of the brain and probably relatively lesser development of the antero-superior part of the frontal lobes compared with the total brain growth rate.

Conclusions

In this paper, we discuss the developmental indicators and the taxonomic affinities of the Mojokerto child. The state of sutural closure on the internal surface of the skull was examined using CT. The anterior fontanelle remains open (Fig. 2) as well as many of the sutures through the cranial bone thickness. Some features such as the cranial bone morphology and the meningeal pattern discrete presence are similar to those observed in very young modern children. Moreover, the cranial bones are thin compared to the adult *Homo erectus* morphology. Meanwhile, the cranial capacity value, the development of osseous superstructures, the presence of a granular foveola and frontal impressions, and the frontal sinuses development, would indicate an older individual age if considering modern human developmental standards. Moreover, the various developmental indicators are apparently in contradiction in this individual, and brain growth pattern in *Homo erectus* appears to be unique. Our data lead us to conclude that this individual was very young, definitely less than 4 years of age (e.g. Risçutia, 1975; Coqueugniot et al., 2001, 2004).

However, It is still impossible to determine precisely its age at death because *Homo erectus* development is still very poorly documented. In the light of our new data, we do not think that modern human growth standards are appropriate to discuss its individual age.

The phyletic status of the Mojokerto child has been considered previously, with different conclusions. The specimen has been classified as *Homo soloensis* (Dubois, 1936), *Australopithecus* (Campbell, 1973), *Pithecanthropus modjokertensis* (Jacob, 1975; Sartono, 1975), *Homo erectus* (e.g. Risçutia, 1975; Storm, 1994; Antón, 1997) or associated with *Homo sapiens* (Weinert, 1938). Many of the Mojokerto child endocranial cast features bring this individual closer to *Homo erectus*: the confluence of sinuses which is different from that observed in most pre *Homo* fossils (Fig. 3, H), the presence of a bulge on the left inferior frontal gyrus (Fig. 3, B) which is developed during hominid evolution, and the prefrontal cortex morphology. The outlines of the inferior surface

of the frontal lobe and of the encephalic rostrum lateral part show a regular curvature. The occipital lobes are located behind the extension of the parietal and temporal lobes. The cerebellar lobes are prominent, separated by a large groove, and located underneath the occipital lobes. These morphological features suggest closest affinities with the Trinil, Sangiran and Zhoukoudian *Homo erectus*. Moreover, because of its endocranial morphology, Mojokerto is more distinct from the Ngandong and Sambungmacan specimens, which are now considered as a particular group of evolved *Homo erectus* (Grimaud-Hervé, 1986, 1997; Balzeau et al., 2002a,b). The information obtained from the endocranial cavity allows us to say that this fossil belongs to *Homo erectus*. Within Javanese *Homo erectus*, precise phyletic or chronological positions are not easily identifiable because of the archaic features of the Mojokerto endocast. Moreover, its young individual age complicates morphological comparisons. The lack of comparative material (the absence of endocranial data for the earlier Javanese hominids, such as Sangiran 27 and 31, or the absence of fossil juvenile individuals) make it impossible to bring the Mojokerto child closer to a particular group of Asian *Homo erectus* if basing arguments on shared archaic features.

However, some features observed on this endocast are similar to those of modern humans. The ascending ramus is slightly tilted forward on the left hemisphere (Fig. 3 RA), the central sulci intersection is anteriorly situated, the endocranial vertex is close to this intersection, so the parietal lobes propagate themselves anteriorly, and the endocast outlines are rounded. On one hand, it appears that this very young *Homo erectus* presents some similarities in its internal characters with adult *Homo sapiens*, and a large brain despite its young age. On the other hand, the presence of a granular foveola (Fig. 3, FG) and numerous digital impressions on the anterior region of the frontal lobes is quite unusual in very young modern humans.

All these evidence concerning the Mojokerto endocranial morphology suggests that *Homo erectus* followed a unique brain growth trajectory. The earliest stages of development, as characterized

by this individual, correspond to an important vertical development and a relative cerebral rounding. Thus the parietal lobes of Mojokerto are relatively more developed than those of adult individuals and the frontal lobes are anteriorly rounded. The ontogeny of *Homo sapiens* presents neotenic retention (Gould, 1977; Deacon, 1990; Begun and Walker, 1993) of ancestral features of its genus, as shown by the shared relative development of the cerebral lobes in Mojokerto and modern humans adults.

The following stages in *Homo erectus* ontogeny correspond to a different growth and development patterns than in *Homo sapiens* (Thompson and Nelson, 2000; Dean et al., 2001). Indeed, the endocranial transformation to an adult morphology occurs by an antero-posterior flattening of the brain. These modifications are particularly characterized by an antero-posterior development of the frontal lobes while the parietal lobes are relatively compressed by the posterior shift of the frontal lobes.

Acknowledgments

We would like to thank Professor E.A. Cabanis – CHNO des Quinze-Vingts, Paris- for the scanning of the fossils, J.T. Richtsmeier for providing the Bosma collection CT data. We thank four anonymous reviewers and the associate editor for their helpful comments. C. Falguères, J. Badawi-Fayad provided invaluable discussions, B.M. Parisi, F. Sémah and R. Macchiarelli helpful comments on earlier versions of this paper. The first author thanks F. Zonneveld for his precious advice. To all of them we are grateful.

References

- Antón, S.C., 1997. Developmental age and taxonomic affinity of the Mojokerto child, Java, Indonesia. *Am. J. Phys. Anthropol.* 102, 497–514.
- Antón, S.C., 2003. Natural history of *Homo erectus*. *Yearb. Phys. Anthropol.* 46, 126–170.
- Baba, H., Aziz, F., Kaifu, Y., Suwa, G., Kono, R.T., Jacob, T., 2003. *Homo erectus* calvarium from the Pleistocene of Java. *Science* 299, 1384–1388.

- Balzeau, A., Jacob, T., Indriati, E., 2002a. Internal cranial features of the Sambungmacan 1 *Homo erectus* (Java, Indonesia). C.R. Palevol 1, 305–310.
- Balzeau, A., Grimaud-Hervé, D., Indriati, E., Jacob, T., Sémah, F., 2002b. Etude comparative de l'endocrâne de l'*Homo erectus* Sambungmacan 3 (Java, Indonésie). Bull. Mém. Soc. Anthropol. Paris 14, 154–155.
- Balzeau, A., Grimaud-Hervé, D., Jacob, T., Sémah, F., Cabanis, E., 2002c. Virtual anthropology: the internal characters of the “Mojokerto child”. Coll. Antropol. 26 (Suppl.), 13.
- Balzeau, A., Indriati, E., Grimaud-Hervé, D., Jacob, T., 2003a. Computer tomography scanning of *Homo erectus* crania Ngandong 7 from Java: internal structure, paleopathology and post-mortem history. B.I. Ked. (J. Med. Sci.) 35, 133–140.
- Balzeau, A., Grimaud-Hervé, D., Indriati, E., Sémah, F., Jacob, T., 2003b. Caractères morphologiques et paléopathologiques crâniens et déformations taphonomiques chez les *Homo erectus* Ngandong 7 et Sangiran 31. Bull. Mém. Soc. Anthropol. Paris 15 (n.s.), 6.
- Beals, K.L., Smith, C.L., Dodd, S.M., 1984. Brain size, cranial morphology, climate, and time machines. Curr. Anthropol. 25, 301–330.
- Begun, D., Walker, A., 1993. The endocast. In: Walker, A., Leakey, R. (Eds.), The Nariokotome *Homo erectus* Skeleton. Springer-Verlag, pp. 326–358.
- Bogin, B., 2003. The human pattern of growth and development in paleontological perspective. In: Thompson, J.L., Krovitz, G.E., Nelson, A.J. (Eds.), Patterns of Growth and Development in the Genus *Homo*. Cambridge University Press, New York, pp. 15–44.
- Bookstein, F.L., Gunz, P., Mitteroecker, P., Prossinger, H., Schaefer, K., Seidler, H., 2003. Cranial integration in *Homo*: singular warps analysis of the midsagittal plane in ontogeny and evolution. J. Hum. Evol. 44, 167–187.
- Bourret, P., Louis, R., 1974. Anatomie du système nerveux central. L'expansion scientifique française, Paris.
- Bräuer, G., Groden, C., Gröning, F., Kroll, A., Kupezik, K., Mbua, E., Pommert, A., Schiemann, T., 2004. Virtual study of the endocranial morphology of the matrix-filled cranium from Eliye Springs, Kenya. Anat. Rec. 276A, 111–133.
- Broadfield, D.C., Holloway, R.L., Mowbray, K., Silvers, A., Yuan, M.S., Márquez, S., 2001. Endocast of Sambungmacan 3 (Sm 3): a new *Homo erectus* from Indonesia. Anat. Rec. 262, 369–379.
- Bruner, E., Averini, M., Manzi, G., 2003. Endocranial traits. Prevalence and distribution in a recent human population. Eur. J. Anat. 7, 23–33.
- Campbell, B.G., 1973. A new taxonomy of fossil man. Yearb. Phys. Anthropol. 17, 194–201.
- Cave, A.J.E., 1961. The frontal sinus of gorilla. Proc. Zool. Soc. Lond. 136, 359–373.
- Conroy, G.C., Vannier, M.W., 1985. Endocranial volume determination of matrix-filled fossil skulls using high-resolution CT. Hominid Revolution: Past, Present and Future. Alan R Liss. pp. 419–426.
- Conroy, G.C., Vannier, M.W., Tobias, P., 1990. Endocranial features of *Australopithecus africanus* revealed by 2 and 3D computed tomography. Science 247, 838–841.
- Conroy, G.C., Weber, G.W., Seidler, H., Tobias, P.V., Kane, A., Brunson, B., 1998. Endocranial capacity in an early hominid from Sterkfontein, South Africa. Science 280, 1730–1731.
- Coqueugnot, H., Hublin, J.-J., Jacob, T., 2001. Révision de l'âge individuel de l'enfant de Modjokerto (Java, Indonésie). XIVe Congrès de l'UISPP, Liège, Belgique.
- Coqueugnot, H., Hublin, J.-J., Veillon, F., Houët, F., Jacob, T., 2004. Early brain growth in *Homo erectus* and implications for cognitive ability. Nature 431, 299–302.
- Deacon, T.W., 1990. Problems of ontogeny and phylogeny in brain size evolution. Int. J. Primatol. 11, 237–282.
- Dean, C., Leakey, M.G., Reid, D., Schrenk, F., Schwartz, G.T., Stringer, C., Walker, A., 2001. Growth processes in teeth distinguish modern humans from *Homo erectus* and earlier hominins. Nature 414, 628–631.
- Delmas, A., Chifflet, J., 1950. Le pressoir d'Hérophyle. C.R. Assoc. Anat. 123–131. 37ème réunion, Louvain.
- Dubois, E., 1894. *Pithecanthropus erectus*, eine menschenähnliche uebergangsform aus Java. Landesdruckerei, Batavia.
- Dubois, E., 1936. Racial identity of *Homo soloensis* Oppenoorth (including *Homo modjokertensis* von Koenigswald) and *Sinanthropus pekinensis* Davidson Black. Proc. Kon. Akd. Wet. Amsterdam 34, 1180–1185.
- Duyfjes, J., 1936. Zur geologie und stratigraphie des Kendengebietes zwischen Trinil und Soerabaja (Java). De Ingenieur in Ned.-Indië. 4, 136–149.
- Falk, D., 1986. Evolution of cranial blood drainage in hominids: enlarged occipital/marginal sinuses and emissary foramina. Am. J. Phys. Anthropol. 70, 311–324.
- Falk, D., Gage, T.B., Dudek, B., Olson, T.R., 1995. Did more than one species of hominid coexist before 3.0 Ma? Evidence from blood and teeth. J. Hum. Evol. 29, 591–600.
- Falk, D., 1998. Hominid brain evolution: looks can be deceiving. Science 280, 1714.
- Falk, D., Redmond Jr., J.C., Guyer, J., 2000. Early hominid brain evolution: a new look at old endocasts. J. Hum. Evol. 38, 695–717.
- Ferembach, D., 1983. Bilan sur la fiabilité des techniques de détermination de l'âge à partir du squelette. Bull. Mém. Soc. Anthropol. Paris 10 (série XIII), 435–440.
- Gabounia, L., Vekua, A., 1995. A Plio-Pleistocene hominid from Dmanisi, East Georgia, Caucasus. Nature 373, 509–512.
- Gabounia, L., Lumley de, M.-A., Vekua, A., Lordkipanidze, D., Lumley de, H., 2002. Découverte d'un nouvel hominidé à Dmanissi (Transcaucasie, Géorgie). C.R. Palevol 1, 243–253.
- Gould, S.J., 1977. Ontogeny and phylogeny. Harvard University Press, Cambridge.
- Grimaud-Hervé, D., 1986. The parietal bone of Indonesian *Homo erectus*. Hum. Evol. 1 (2), 167–182.
- Grimaud-Hervé, D., 1994. Evolution of the Javanese fossil hominid brain. Cour. Forsch.-Inst. Senckenberg 171, 61–68.

- Grimaud-Hervé, D., 1997. L'évolution de l'encéphale chez l'*Homo erectus* et l'*Homo sapiens*: exemples de l'Asie et de l'Europe. Cahiers de paléanthropologie. CNRS, Paris.
- Hauser, G., de Stefano, G.F., 1989. Epigenic variants of the human skull. E. Schweizerbart'sche Verlagsbuchhandlung, Stuttgart.
- Hershkovitz, I., Latimer, B., Dutour, O., Jellema, L.M., Wish-Baratz, S., Rothschild, B.M., 1997. Why do we fail in aging the skull from the sagittal suture? *Am. J. Phys. Anthropol.* 103, 393–399.
- Holloway, R.L., 1973. New endocranial values for the East African early hominids. *Nature* 243, 97–99.
- Holloway, R.L., 1978. Problems of brain endocast interpretation and African hominid evolution. In: Jolly, C.J. (Ed.), *Early Hominids of Africa*. St Martin's Press, New York, pp. 379–401.
- Holloway, R.L., 1981. The Indonesian *Homo erectus* brain endocast revisited. *Am. J. Phys. Anthropol.* 55, 503–521.
- Holloway, R.L., 1983a. Human brain evolution: a search for units, models and synthesis. *Can. J. Anthropol.* 3, 215–230.
- Holloway, R.L., 1983b. Human paleontological evidence relevant to language behavior. *Hum. Neurobiol.* 2, 105–114.
- Hublin, J.J., Spoor, F., Braun, M., Zonneveld, F., Condemi, S., 1996. A late Neanderthal with upper Palaeolithic artefacts. *Nature* 381, 224–226.
- Huffman, O.F., 2001. Geologic context and age of the Pening/Mojokerto *Homo erectus*, East Java. *J. Hum. Evol.* 40, 353–362.
- Huffman, O.F., Zaim, Y., 2003. Mojokerto Delta, East Java: Paleoenvironment of *Homo modjokertensis*, first results. *J. Miner. Technol.* 10 (2) The Faculty of Earth Sciences and Mineral Technology, Institute Technology, Bandung.
- Hyodo, M., Watanabe, N., Sunata, W., Susanto, E.E., Wahyono, H., 1993. Magnetostratigraphy of hominid fossil bearing formations in Sangiran and Mojokerto, Java. *Anthropol. Sci.* 101 (2), 157–183.
- Hyodo, M., Nakaya, H., Urabe, A., Saegusa, H., Shunrong, X., Jiyun, Y., Xuepin, J., 2002. Paleomagnetic dates of hominid remains from Yuanmou, China, and other Asian sites. *J. Hum. Evol.* 43, 27–41.
- Jacob, T., 1966. The sixth skull cap of *Pithecanthropus erectus*. *Am. J. Phys. Anthropol.* 25, 243–260.
- Jacob, T., 1975. Morphology and paleoecology of early Man in Java. In: Tuttle, R.H. (Ed.), *Paleoanthropology, Morphology and Paleoecology*. Mouton, The Hague, pp. 321–325.
- Kamina, P., Renard, M., 1994. Tête osseuse, articulation temporo-mandibulaire et dents. Maloine.
- von Koenigswald, G.H.R., 1936. Ein fossiler hominide aus dem Altpleistocän Ostjawas. *De Ingenieur in Ned.-Indië.* 8, 149–158.
- von Koenigswald, G.H.R., 1940. neue *Pithecanthropus* funde. Landsdrukkerij, Batavia.
- Koppe, T., Ohkawa, Y., 1999. Pneumatization of the facial skeleton in Catarrhine primates. In: Koppe, T., Nagai, H., Alt, K.W. (Eds.), *The Paranasal Sinuses of Higher Primates: Development, Function and Evolution*. Quintessence, Chicago, pp. 77–120.
- Libersa, C., Faber, M., 1960. Pneumatization de la tête du cornet moyen. *J. Otorhinolaryngol.* 6, 723–740.
- Maitrerobert, A., 2002. L'origine du langage articulé, le tractus vocal et ses relations avec la base du crâne et de la mandibule. Thèse de doctorat, Muséum national d'Histoire naturelle.
- Masset, C., 1971. Erreurs systématiques dans la détermination de l'âge par les sutures crâniennes. *Bull. Mem. Soc. Anthropol. Paris* 7 (série XII), 85–105.
- Minugh-Purvis, N., Radovic, J., Smith, F.H., 1999. Krapina 1: a juvenile Neandertal from the early late Pleistocene of Croatia. *Am. J. Phys. Anthropol.* 111, 393–424.
- Paturet, G., 1951. *Traité d'anatomie humaine, ostéologie, anthropologie-myologie*. Tome I. Masson., Paris.
- Ponce de León, M.S., Zollikofer, C.P.E., 2001. Neandertal cranial ontogeny and its implications for late hominid diversity. *Nature* 412, 534–538.
- Prossinger, H., Seidler, H., Wicke, L., Weaver, D., Recheis, W., Stringer, C., Muller, G., 2003. Electronic removal of encrustations inside the Steinheim cranium reveals paranasal sinus features and deformations, and provides a revised endocranial volume estimate. *Anat. Rec.* 273B, 132–142.
- Recheis, W., Macchiarelli, R., Seidler, H., Weaver, D., Schäfer, K., Bondioli, L., Weber, G.W., zur Nedden, D., 1999. Re-evaluation of the endocranial volume of the Guattari 1 Neandertal specimen. *Coll. Antropol.* 23 (2), 397–405.
- Risçutia, C., 1975. A study on the Modjokerto infant calvarium. In: Tuttle, R.H. (Ed.), *Paleoanthropology, Morphology and Paleoecology*. Mouton, The Hague, pp. 373–375.
- Rook, L., Bondioli, L., Casali, F., Rossi, M., Kohler, M., Moya Sola, S., Macchiarelli, R., 2004. The bony labyrinth of *Oreopithecus bambolii*. *J. Hum. Evol.* 46, 347–354.
- Ruff, C.B., Leo, F.P., 1986. Use of computed tomography in skeletal structure research. *Am. J. Phys. Anthropol.* 29, 181–196.
- Rushton, J.P., 1997. Cranial size and IQ in Asian Americans from birth to age seven. *Intelligence* 25, 7–20.
- Saban, R., 1988. Le réseau méningé dans les crânes déformés: déformation toulousaine et déformation péruvienne. *Soc. d'études rech. préhist., Les Eyzies* 37, 99–120.
- Saban, R., 1993. *Aux sources du langage*. Masson, Paris. collection Préhistoire.
- Sartono, S., 1975. Implications arising from *Pithecanthropus* VIII. In: Tuttle, R.H. (Ed.), *Paleoanthropology, Morphology and Paleoecology*. Mouton, The Hague, pp. 327–360.
- Scheuer, L., Black, S., 2000. *Developmental juvenile osteology*. Academic Press, San Diego.
- Schwartz, G.T., Thackeray, J.F., Reid, C., Van Reenan, J.F., 1998. Enamel thickness and the topography of the enamel-dentine junction in South Africa Plio-Pleistocene hominids with special reference to the Carabelli trait. *J. Hum. Evol.* 35, 523–542.
- Sémah, F., 1986. Le peuplement ancien de Java. *Chronologie. L'anthropologie* 90, 359–400.

- Shapiro, D., Richtsmeier, J.T., 1997. Brief communication: a sample of pediatric skulls available for study. *Am. J. Phys. Anthropol.* 103, 415–416.
- Silcox, M.T., 2003. New discoveries on the middle ear anatomy of *Ignacius graybullianus* (Paromomyidae, Primates) from ultra high resolution X-ray computed tomography. *J. Hum. Evol.* 44, 73–86.
- Spoor, F., Zonneveld, F., Macho, G.A., 1993. Linear measurements of cortical bone and dental enamel by CT: applications and problems. *Am. J. Phys. Anthropol.* 91, 469–484.
- Spoor, F., Jeffery, N., Zonneveld, F., 2000. Imaging skeletal growth and evolution. In: O'Higgins, P., Cohn, M. (Eds.), *Development, Growth and Evolution: Implications for the Study of the Hominid Skeleton*. Academic press, London, pp. 123–161.
- Spoor, F., Hublin, J.J., Braun, M., Zonneveld, F., 2003. The bony labyrinths of Neanderthals. *J. Hum. Evol.* 44, 141–165.
- Storm, P., 1994. De morfologie van *Homo modjokertensis*. *Cranium* 11, 97–102.
- Stringer, C.B., 1986. The credibility of *Homo habilis*. In: Wood, B., Martin, L., Andrews, P. (Eds.), *Major Topics in Primate and Human Evolution*. Cambridge University Press, Cambridge, pp. 266–294.
- Swisher III, C.C., Curtis, G.H., Jacob, T., Getty, A.G., Suprijo, A., Widiasmoro, 1994. Age of the earliest known hominids in Java, Indonesia. *Science* 263, 1118–1121.
- Tate, J.R., Cann, C.E., 1982. High-resolution computed tomography for the comparative study of fossil and extant bone. *Am. J. Phys. Anthropol.* 58, 67–73.
- Terra, H.de, 1938. Fourth scientific field report of the American southeast Asiatic expedition for cenozoic geology and early man, Academy of Natural Sciences of Philadelphia, the Peabody museum of Harvard University, and Carnegie Institution of Washington. Report on file (9 pages; collection 113 IV No. 6), Carnegie Institution of Washington, Washington D.C.
- Thompson, J.L., Nelson, A.J., 2000. The place of Neanderthals in the evolution of hominid patterns of growth and development. *J. Hum. Evol.* 38, 475–495.
- Tobias, P.V., 1975. Brain evolution in the Hominoidea. In: Tuttle, R.H. (Ed.), *Primate Functional Morphology and Evolution*. Mouton, The Hague, pp. 353–392.
- Tobias, P.V., 1983. Recent advances in the evolution of the hominids with especial reference to brain and speech. In: Chagas, C. (Ed.), *Recent Advances in the Evolution of Primates*. Pontifica Academia Scientiarum, Citta del Vaticano, pp. 85–140.
- Tobias, P.V., 1987. The brain of *Homo habilis*: a new level of organization in cerebral evolution. *J. Hum. Evol.* 16, 741–761.
- Tobias, P.V., Falk, D., 1988. Evidence for a dual pattern of cranial venous sinuses on the endocranial cast of Taung (*Australopithecus africanus*). *Am. J. Phys. Anthropol.* 76, 309–312.
- Tobias, P.V., 2001. Re-creating ancient hominid virtual endocasts by CT-scanning. *Clin. Anat.* 14, 134–141.
- Vannier, M.W., Conroy, G.C., Marsh, J.L., Knapp, R.H., 1985. Three-dimensional cranial surface reconstructions using high-resolution computed tomography. *Am. J. Phys. Anthropol.* 67, 299–311.
- Vekua, A., Lordkipanidze, D., Rightmire, G.P., Agusti, J., Ferring, R., Maisuradze, G., Mouskhelishvili, A., Nioradze, M., Ponce de Leon, M., Tappen, M., Tvalchrelidze, M., Zollikofer, C., 2002. A new skull of early *Homo* from Dmanissi, Georgia. *Science* 297, 85–89.
- Weinert, H., 1938. *Entstehung Der Menschrassen*. Ferdinand Enke Verlag, Stuttgart.
- Weinmann, J.P., Sicher, H., 1955. *Bone and bones: fundamentals of bone biology*, second ed. Kimpton, London.
- Wind, J., 1984. Computerized X-Ray tomography of fossil hominid skulls. *Am. J. Phys. Anthropol.* 63, 265–282.
- Zihlman, A., Bolter, D., Boesch, C., 2004. Wild chimpanzee dentition and its implications for assessing life history in immature hominin fossils. *Proc. Nat. Acad. Sci.* 101, 10541–10543.
- Zonneveld, F., Wind, J., 1985. High-resolution CT of fossil hominid skulls: a new method and some results. *Hominid Revolution: Past, Present and Future*. Alan R Liss. pp. 427–436.